MOLECULAR AND CELLULAR BIOLOGY, Dec. 2005, p. 10507–10515 Vol. 25, No. 23
0270-7306/05/$08.00+0 doi:10.1128/MCB.25.23.10507–10515.2005

H3 Lysine 9 Methylation Is Maintained on a Transcribed Inverted Repeat by Combined Action of SUVH6 and SUVH4 Methyltransferases

Michelle L. Ebbs, Lisa Bartee, and Judith Bender*

Department of Biochemistry and Molecular Biology, Johns Hopkins University Bloomberg School of Public Health, 615 N. Wolfe St., Baltimore, Maryland 21205

Received 30 August 2005/Accepted 12 September 2005

Transcribed inverted repeats are potent triggers for RNA interference and RNA-directed DNA methylation in plants through the production of double-stranded RNA (dsRNA). For example, a transcribed inverted repeat of endogenous genes in *Arabidopsis thaliana*, *PAI1-PAI4*, guides methylation of itself as well as two unlinked duplicated *PAI* genes, *PAI2* and *PAI3*. In previous work, we found that mutations in the SUVH4/KYP histone H3 lysine 9 (H3 K9) methyltransferase cause a loss of DNA methylation on *PAI2* and *PAI3*, but not on the inverted repeat. Here we use chromatin immunoprecipitation analysis to show that the transcribed inverted repeat carries H3 K9 methylation, which is maintained even in an *suvh4* mutant. *PAI1-PAI4* H3 K9 methylation and DNA methylation are also maintained in an *suvh6* mutant, which is defective for a gene closely related to *SUVH4*. However, both epigenetic modifications are reduced at this locus in an *suvh4 suvh6* double mutant. In contrast, SUVH6 does not play a significant role in maintenance of H3 K9 or DNA methylation on *PAI2*, transposon sequences, or centromere repeat sequences. Thus, SUVH6 is preferentially active at a dsRNA source locus versus targets for RNA-directed chromatin modifications.

In eukaryotic genomes, condensed transcriptionally silent heterochromatin domains serve key roles in gene regulation and genome stability. In mammals and plants, heterochromatin is associated with cytosine methylation, as well as with histone tail modifications including H3 methylated at lysine 9 (H3 mK9). In many cases, these heterochromatin-associated modifications are directed to target sequences by a double-stranded RNA (dsRNA)-derived signal (26). For example, in plants, sources of dsRNA that can be converted into small RNAs by dicer RNase action, such as RNA viruses, products of RNA-dependent RNA polymerase synthesis, or transcripts derived from inverted repeat templates, direct DNA methylation and H3 mK9 of identical genomic sequences. However, the factors that connect RNA signals with DNA methylation and H3 mK9 remain to be elucidated.

Plant RNA-directed DNA methylation typically affects cytosines in all sequence contexts (26). Genetic studies in *Arabidopsis thaliana* indicate that methylation in the symmetric context 5′ CG 3′ is maintained by the MET1 cytosine methyltransferase (MTase) (16, 37). Maintenance of methylation in non-CG contexts is more complex, with contributions from both the DRM1/DRM2 and CMT3 cytosine MTases. DRM1 and DRM2 control the initiation of new methylation imprints (7) but have different roles in the maintenance of non-CG methylation at different genomic regions (6). For example, although DRM1 and DRM2 are required to maintain non-CG methylation at direct repeat sequences that lie 3′ to the *MEA* gene, they do not obviously contribute to maintenance of non-CG methylation at the *Ta3* retrotransposon or at centromere-associated repeats. Instead, CMT3 is the major enzyme involved in maintenance of non-CG methylation at these targets (2, 6, 20), as well as at other transposon sequences (17, 23, 41).

Like mutations in CMT3, mutations in the SUVH4/KYP (hereafter referred to as SUVH4) H3 K9 MTase cause a loss of non-CG methylation on target sequences including centromere repeats and transposons (11, 23, 25). This finding suggests that CMT3 is guided to target sequences by SUVH4-mediated H3 mK9. Similarly, in *Neurospora crassa*, H3 mK9 is needed for DNA methylation mediated by the Dim-2 cytosine MTase (18, 39), and mutations in mammalian H3 K9 MTases cause loss of DNA methylation from specific genomic regions (19, 44). However, *Arabidopsis suvh4* mutations confer weaker demethylation phenotypes than *cmt3* mutations do. For example, centromere repeats and transposon sequences show only a partial loss of non-CG methylation in *suvh4* mutant backgrounds versus *cmt3* mutant backgrounds (11, 23, 25). A possible explanation is that histone MTases besides SUVH4 contribute to H3 mK9 maintenance at CMT3 targets. In support of this view, the *Arabidopsis* genome encodes eight other SUVH [*Su*(*v*ar)3-9 *h*omologue] predicted H3 K9 MTases (3), and the SUVH6 enzyme has been shown to have similar H3 dimethyl K9 activity to SUVH4 in vitro (10). Furthermore, mass spectrometry analysis of H3 modifications indicates that the *suvh4* mutant retains residual H3 mK9 (15).

Although loss of H3 mK9 causes loss of CMT3-mediated non-CG methylation, in some cases loss of DNA methylation causes loss of H3 mK9. For example, mutations in the MET1 CG MTase deplete H3 mK9 from centromere repeats and transposon sequences (23, 38, 40). This depletion of H3 mK9 might occur as an indirect consequence of transcriptional reactivation induced by DNA demethylation (14). Alternatively, DNA methylation, particularly in CG contexts, might act as a

* Corresponding author. Mailing address: Department of Biochemistry and Molecular Biology, Johns Hopkins University Bloomberg School of Public Health, 615 N. Wolfe St., Baltimore, MD 21205. Phone: (410) 614-1595. Fax: (410) 955-2926. E-mail: jbender@mail.jhmi.edu.

reinforcing mechanism to recruit the factors involved in non-CG methylation, including RNA effector complexes and histone methyltransferases, to heterochromatin targets.

The endogenous duplicated *PAI* tryptophan biosynthetic genes provide a model system to study RNA-directed non-CG methylation maintained by H3 mK9 and CMT3. In the Wasilewskija (WS) strain background, the *PAI* genes are arranged as a tail-to-tail inverted repeat of two genes, *PAI1-PAI4* and two unlinked singlet genes, *PAI2* and *PAI3*, and all four genes are densely methylated at both CG and non-CG residues (24, 30). The *PAI1-PAI4* inverted repeat is transcribed from a fortuitous promoter that lies in the unmethylated region upstream of *PAI1*, producing both normally polyadenylated *PAI1* transcripts and longer read-through transcripts into palindromic *PAI4* sequences (29). Thus, *PAI1-PAI4* produces a direct source of dsRNA that can potentially be processed and recruit heterochromatin effector proteins at the site of transcription for very efficient DNA methylation of the locus. Consistent with this view, when transcription of the locus is suppressed by targeted methylation of the upstream promoter in a transgenic derivative of WS, WS(S15aIR), *PAI2* and *PAI3* lose non-CG methylation, while *PAI1-PAI4* maintains full methylation (29). *PAI2* and *PAI3* also lose non-CG methylation but retain CG methylation when the *PAI1-PAI4* locus is eliminated from the genome (4, 13, 24), indicating that the CG MTase MET1 can maintain *PAI* CG methylation even in the absence of an RNA signal.

In previous work we found that mutations in CMT3 cause an almost complete loss of non-CG methylation from all three *PAI* loci (2). In contrast, mutations in SUVH4 cause a loss of non-CG methylation on *PAI2* and *PAI3* but do not affect DNA methylation at the *PAI1-PAI4* dsRNA source locus (25). Here we show that *PAI1-PAI4* maintains H3 mK9 despite transcription of the locus through the combined action of SUVH4 and the related protein SUVH6: only in an *suvh4 suvh6* double mutant is the locus depleted for H3 mK9 and non-CG methylation. In contrast, SUVH6 does not play a significant role in maintenance of H3 mK9 and non-CG methylation on *PAI2*, transposon sequences, and centromere repeat sequences. Thus, SUVH6 contributes to H3 mK9 and DNA methylation in vivo with preferential activity at the *PAI1-PAI4* transcribed inverted repeat.

MATERIALS AND METHODS

Plant strains. The Columbia (Col) *suvh6-1* T-DNA insertion mutation was obtained from the Syngenta mutant collection (27). The left border insertion junction lies 1,576 base pairs downstream from the ATG translational start codon of *SUVH6* in the center of the pre-SET portion of the catalytic sequences. Col *suvh6-1* was crossed with WS *pai1* (1), and PCR-based genotype markers were used to identify four independent progeny that were homozygous WS at each of the three *PAI* loci (24) and homozygous for the *suvh6-1* mutation. PCR primers to amplify the transgene insertion are LB3 5′ TAGCATCTGAATTTC ATAACCAATCTCGATACAC 3′ and SUVH6GAR1 5′ CCTGTGCGAAGA ACATCACGTG 3′, which yield a 789-bp product; PCR primers to amplify the intact *SUVH6* gene are SUVH6GAR1 and SUVH6F3 5′ CTGAAAGAGCCT GAAGACC 3′, which amplify a 1,015-bp product. Col *suvh6-1* was also crossed with WS *pai1 suvh4R302** (25), and PCR-based genotype markers were used to identify three independent progeny that were homozygous WS at each of the three *PAI* loci, homozygous for the *suvh4R302** mutation, and homozygous for the *suvh6-1* mutation. Southern blot assays for *PAI* and transposon DNA methylation were used to determine that the phenotypes of four independent *pai1 suvh6-1* lines were similar to each other and that the phenotypes of three independent *pai1 suvh4 suvh6-1* lines were similar to each other. Thus, it is unlikely that modifier loci influencing DNA methylation of *PAI* and transposon sequences are segregating in the WS/Col hybrid backgrounds. Bisulfite genomic sequencing of *PAI* DNA methylation patterns (see Fig. 4B) and chromatin immunoprecipitation (ChIP) analysis (see Fig. 3) were performed on one representative line of each *suvh* genotype.

The *cmt3 met1* double mutant was constructed by crossing WS *pai1 cmt3illa* (2) with the *met1-1* allele (16) crossed into a WS background (WS *met1* [1]). Two independent progeny with a WS *pai1 cmt3illa met1-1* genotype were identified, with a representative line used for the experiments shown in Fig. 1 and 2 and for bisulfite sequencing of *PAI* methylation patterns. In contrast to the *pai1 met1-1* (1) and *pai1 cmt3illa* (2) mutants, which retain fluorescence diagnostic of *PAI2* silencing, the *pai1 cmt3ill1 met1-1* mutant lines were completely nonfluorescent. The nonfluorescent phenotype is diagnostic of full transcriptional reactivation of *PAI2* (4, 13).

ChIP analysis. ChIP assays were performed using a previously described method (9) starting with 0.7 g of leaf tissue from 3-week-old plants grown in soilless potting mix (Fafard mix 2) under continuous illumination. Chromatin was immunoprecipitated with anti-H3 dimethyl K4 antibodies (Upstate Biotechnologies) or with anti-H3 dimethyl K9 antibodies (gift of T. Jenuwein, Vienna Biocenter) or carried through the protocol with no antibody added as a control (mock precipitation, see Fig. 2 and 3). Gene-specific PCR primer sets that amplify fragments of approximately 100 bp were designed for each *PAI* gene taking advantage of regions of sequence polymorphisms: for *PAI2* and *PAI3* the amplified region lies at the junction of the first intron and second exon, for *PAI1* the amplified region lies at the 3′ end of the gene at the junction with palindromic *PAI4* sequences, and for *S15a* the amplified region lies at the duplicated *S15a* transcription start sites (see Fig. 1A). ChIP primer sequences used in this study are available upon request.

PCR was performed on ChIP samples using the following PCR program: 94°C for 5 min, followed by 24 to 32 cycles, with 1 cycle consisting of 94°C for 15 seconds and 60°C for 60 seconds. For all primer sets except the *AtMu1* set, which amplifies a 161-bp product (longer than any of the other ChIP PCR products assayed in this study), the mK4 samples were amplified for 24 cycles, the input samples were amplified for 26 cycles, and the mK9 and mock samples were amplified for 28 cycles. For *AtMu1*, mK4 and input samples were amplified for 28 cycles and mK9 and mock samples were amplified for 32 cycles. PCR-amplified products from ChIP template DNA were visualized on a 2.5% agarose gel stained with GelStar (Cambrex). Each ChIP assay was performed in three independent experiments, with results from a representative experiment shown in Fig. 2 and 3.

Sodium bisulfite genomic sequencing of DNA methylation patterning. Bisulfite sequencing of the top strands of the *PAI1* and *PAI2* proximal promoter regions was performed on DNA prepared from representative lines of WS *pai1 suvh6-1*, WS *pai1 suvh4 suvh6-1*, or *pai1 cmt3 met1* as previously described (29) with eight clones per locus sequenced. The compiled data for the *suvh* mutant strains are shown in Fig. 4B. For *pai1 cmt3 met1* bisulfite sequencing, at *PAI1* none of 520 monitored cytosines was methylated, and at *PAI2* one out of 512 monitored cytosines was methylated.

RESULTS

The *PAI1-PAI4* transcribed inverted repeat maintains H3 mK9 in wild-type and *suvh4* backgrounds. The *PAI1-PAI4* transcribed inverted repeat maintains full DNA methylation in the *suvh4* mutant, but it loses non-CG methylation in the *cmt3* mutant relative to the wild-type WS (25) (Fig. 1). A possible explanation for this observation is that SUVH4 acts redundantly with other H3 K9 MTases at *PAI1-PAI4* to make the H3 mK9 modification that guides CMT3. To test this possibility, we performed ChIP assays for H3 mK9, as well as the H3 methyl-lysine 4 (H3 mK4) modification associated with transcribed unmethylated genes in *Arabidopsis* (9, 22, 23), on the *PAI* genes in the wild-type WS versus the *suvh4* mutant.

We also performed ChIP assays on *cmt3* and *cmt3 met1* DNA MTase mutants to understand how the H3 modifications change in response to altered *PAI* DNA methylation. In the *cmt3 met1* double mutant strain, all three *PAI* loci are nearly completely demethylated in both CG and non-CG contexts as

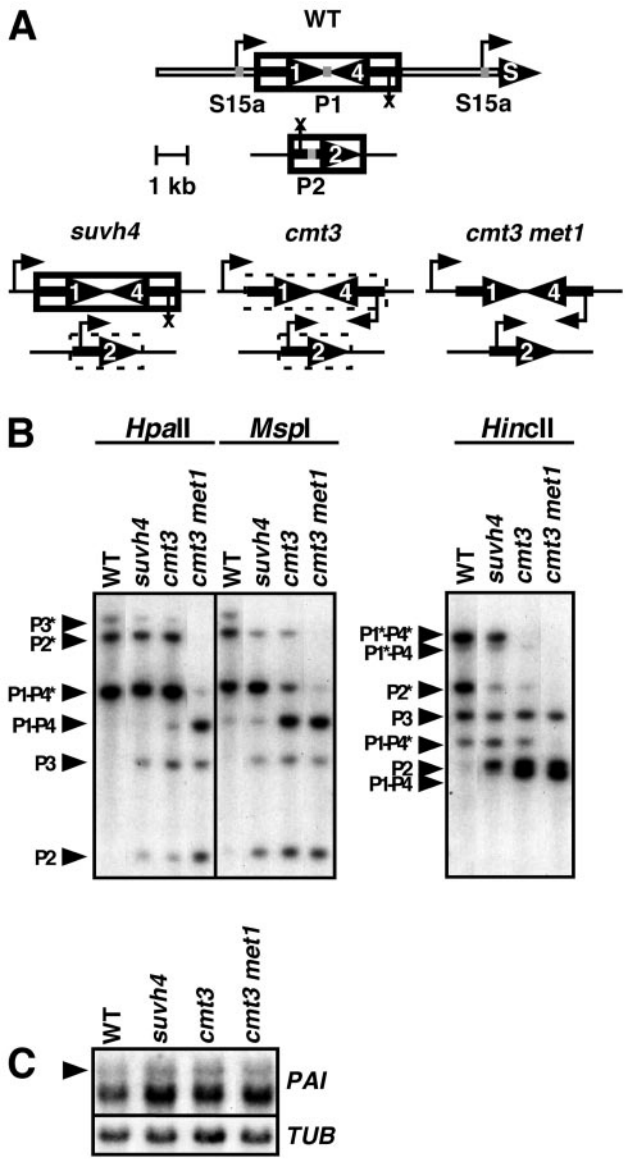

FIG. 1. *PAI* gene DNA methylation patterning and transcriptional activity in DNA methylation-deficient mutants. (A) Diagram summary of DNA methylation patterns and transcriptional activity for *PAI1-PAI4* and *PAI2*. Each *PAI* sequence (labeled 1, 2, or 4), including regions of identity upstream and downstream of the coding region, or the *S15a* gene (labeled S) is indicated by a thick black arrow. The 2.9-kb unmethylated direct repeat regions flanking *PAI1-PAI4* are indicated by open bars. Regions of DNA methylation are shown boxed by a solid line for CG and non-CG methylation or by a dashed line for CG methylation. An arrow indicates transcription, and an X indicates silencing. Sites of PCR amplification used for ChIP analysis are indicated with gray bars on the diagram for wild-type WS (WT), with P1 indicating the *PAI1* site, P2 indicating the *PAI2* site, and S15a indicating the *S15a* transcription start sites. (B) Southern blot assays for *PAI* DNA methylation patterning. Genomic DNA from the indicated strains was cleaved with HpaII, MspI, or HincII and used in Southern blot analysis with a *PAI1* cDNA probe. P1-P4 indicates *PAI1-PAI4*, P2 indicates *PAI2*, and P3 indicates *PAI3*, with bands diagnostic of methylation on *PAI*-internal sites denoted with asterisks. (C) *PAI1* transcript levels are not significantly altered by changes in internal DNA methylation patterns at the *PAI1-PAI4* transcribed inverted repeat. Total RNA was isolated from 3-week-old plants of the indicated strains and used to prepare duplicate gel blots that were probed with a *PAI1* cDNA probe (*PAI*) or a β-tubulin (*TUB*) probe as a loading control.

determined by Southern blot assay (Fig. 1B) and bisulfite genomic sequencing (Materials and Methods). For Southern blot analysis, genomic DNA was digested with HpaII, MspI, or HincII. HpaII and MspI recognize 5′ CCGG 3′, with HpaII inhibited by methylation of either cytosine (CG or CCG) and MspI inhibited by methylation only of the outer cytosine (CCG) (outer cytosine underlined). These enzymes have a single internal methylated recognition site at each WS *PAI* locus (4). The HincII digest monitors methylation of a cytosine in the context of 5′ CAG 3′ on one strand and 5′ CAT 3′ on the other strand of the recognition site in *PAI* sequences. HincII has single internal methylated recognition sites at the translational start codons of *PAI1*, *PAI4*, and *PAI2*, but not *PAI3* due to a polymorphism (25). We did not include WS *met1* in our ChIP analysis because this strain retains substantial CG methylation as well as non-CG methylation on the *PAI* genes and is overall only weakly demethylated relative to WS (1). Figure 1A summarizes the *PAI* methylation patterns and transcriptional activity in the four strains used in ChIP analysis.

In wild-type WS, *PAI1-PAI4* was enriched for H3 mK9 (Fig. 2A), demonstrating that H3 K9 MTases are recruited to this locus despite its transcription. Furthermore, full H3 mK9 was maintained in an *suvh4* background relative to WS, indicating that H3 K9 MTases other than SUVH4 act efficiently at this locus. Below we show that SUVH6 and SUVH4 both control H3 mK9 at *PAI1-PAI4*.

In the *cmt3* DNA MTase mutant background where *PAI1-PAI4* is demethylated in non-CG contexts (2) (Fig. 1), H3 mK9 was maintained at similar levels in the wild type and *suvh4* mutant (Fig. 2A). However, the H3 mK9 modification was lost in the *cmt3 met1* double DNA MTase mutant where the locus is demethylated in both CG and non-CG contexts. A possible explanation for the loss of H3 mK9 from *PAI1-PAI4* in the *cmt3 met1* double mutant is that this locus is transcriptionally hyperactivated relative to the wild type and to *suvh4* and *cmt3* single mutants. However, RNA gel blot analysis showed similar accumulation of *PAI1* transcripts as monitored by an approximately 1,900-nucleotide (nt) splice variant unique to the *PAI1* gene (28) in all four strains (Fig. 1C), arguing against this mechanism of H3 mK9 loss. Furthermore, the H3 mK4 mark associated with transcriptional activation was not elevated in the *cmt3 met1* mutant relative to the other strains tested. Instead, the loss of *PAI1-PAI4* H3 mK9 uniquely in the *cmt3 met1* background might reflect a direct requirement for DNA methylation to maintain H3 mK9 at transcribed but DNA methylated loci.

In all four backgrounds, only a low level of H3 mK4 was detected at *PAI1-PAI4*, even though H3 mK4 is normally enriched on transcribed genes (for example, see *Actin* in Fig. 2E).

Four strains were used; WT is wild type WS, *suvh4* is WS *suvh4R302** (25), *cmt3* is WS *cmt3i11a* (2), and *cmt3 met1* is *pai1 cmt3i11a met1-1* (Materials and Methods). The arrowhead in the left margin indicates the position of a 1,900-nt 5′ splice variant unique to *PAI1* (28). Note that in the wild-type WS the major *PAI* transcript pool consists of two other *PAI1* 5′ splice variants that are both approximately 1,200 nt. In the three mutant backgrounds where additional *PAI* genes are demethylated, *PAI* transcripts initiating in proximal *PAI* promoter sequences also give rise to approximately 1,200-nt transcripts that contribute to the intensity of the smaller-molecular-size pool.

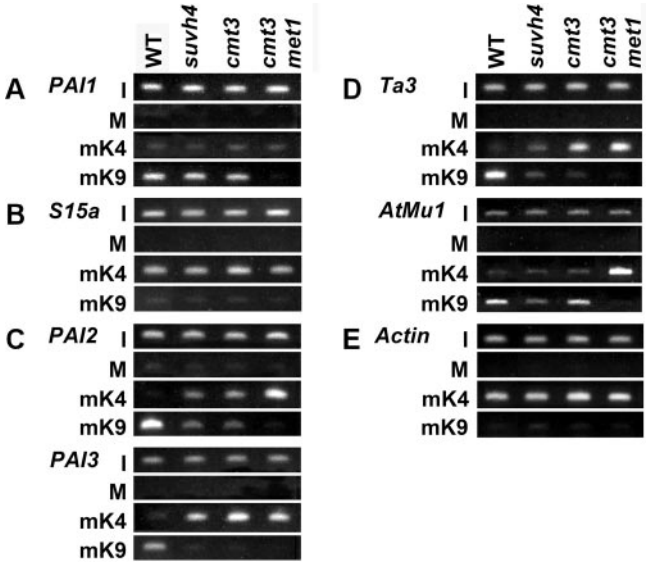

FIG. 2. *PAI* gene H3 mK4 and H3 mK9 patterning in DNA methylation-deficient mutants. Primer sets specific for (A) the *PAI-PAI4* transcribed inverted repeat, (B) the unmethylated *S15a* transcription start regions flanking the *PAI1-PAI4* inverted repeat, (C) the *PAI2* and *PAI3* targets for *PAI1-PAI4* RNA-directed DNA methylation, (D) the *Ta3* retrotransposon and *AtMu1* DNA transposon, and (E) the unmethylated transcribed *Actin* gene were used to amplify PCR products from total input chromatin (I), no-antibody mock precipitation control (M), chromatin immunoprecipitated with H3 anti-dimethyl K4 antibodies (mK4), or chromatin immunoprecipitated with H3 anti-dimethyl K9 antibodies (mK9) from the indicated strains. Four strains were used: WT is wild-type WS, *suvh4* is WS *suvh4R302** (25), *cmt3* is WS *cmt3i11a* (2), and *cmt3 met1* is *pai1 cmt3i11a met1-1* (Materials and Methods). GelStar-stained PCR products are shown. These results were reproduced in three independent experiments, with a representative data set shown.

The transcription start site of the *PAI-PAI4* inverted repeat maintains H3 mK4. The DNA methylated *PAI1-PAI4* inverted repeat is flanked by 2.9-kilobase unmethylated direct repeat duplications that include the promoter, first exon, and first intron of the *S15a* putative ribosomal protein-encoding gene (29) (Fig. 1A). One copy of the *S15a* promoter region is fused to the proximal promoter sequences of *PAI1* and drives transcription through the *PAI1-PAI4* inverted repeat. The other copy of the *S15a* promoter region lies distal to *PAI4* and drives transcription of the *S15a* gene. We used ChIP analysis to monitor the histone methylation status of the *S15a* transcription start site region to determine whether the H3 mK9 enrichment detected in the DNA methylated portion of the *PAI1-PAI4* inverted repeat extends into the flanking unmethylated transcribed sequences.

In the wild-type WS background, the *S15a* loci maintained H3 mK4 with only a low level of H3 mK9 (Fig. 2B). This pattern was unaffected in the *suvh4*, *cmt3*, and *cmt3 met1* mutant backgrounds. These results suggest that both copies of the *S15a* transcription start region are primarily modified by H3 mK4 and that H3 mK9 enrichment is confined to the DNA methylated portion of *PAI1-PAI4*.

Transcriptionally reactivated *PAI* genes show a loss of H3 mK9 and a gain of H3 mK4. The singlet *PAI2* and *PAI3* genes are targets of the dsRNA signal for DNA methylation produced from *PAI1-PAI4* (29). In wild-type WS, both genes are fully DNA methylated over their regions of identity with *PAI1-PAI4*: *PAI2* identity/methylation extends for approximately 250 bp upstream of the transcription start, whereas *PAI3* identity/methylation begins near the transcription start site (24, 30). *PAI2* and *PAI3* are demethylated at non-CG residues in *suvh4* and *cmt3* backgrounds (2, 25) and are demethylated in all contexts in the *cmt3 met1* background (Fig. 1) (Materials and Methods). On the basis of the phenotypes of a reporter strain for *PAI2* activity, *PAI2* is transcriptionally silent in the wild type, partially transcriptionally reactivated in *suvh4* and *cmt3* mutants, and fully transcriptionally reactivated in the *cmt3 met1* mutant (25) (Materials and Methods). The *PAI2* transcription patterns are thus consistent with the proximal promoter DNA methylation patterns. *PAI3* is expressed at only a low level even when unmethylated and does not encode functional PAI enzyme, making it difficult to monitor its transcriptional activity against the background of *PAI1* expression in WS (30). However, because *PAI3* has only four CG cytosines in the *PAI*-identical promoter/first exon region targeted for DNA methylation (24), it is likely that the gene is strongly transcriptionally reactivated by mutations that block non-CG methylation. It should also be noted that *PAI3* is only approximately 90% identical to the other three WS *PAI* genes due to a number of polymorphisms; perhaps because of this reduced sequence identity, *PAI3* is less efficiently targeted for DNA methylation by *PAI1-PAI4* dsRNA than is *PAI2* (24).

ChIP analysis showed that *PAI2* and *PAI3* were modified with H3 mK9 but not H3 mK4 in wild-type WS (Fig. 2C). However, both singlet *PAI* genes lost H3 mK9 and acquired H3 mK4 in *suvh4*, *cmt3*, and *cmt3 met1* mutant backgrounds. *PAI2* displayed a partial reduction in H3 mK9 and a partial gain of H3 mK4 in *suvh4* and *cmt3* mutants relative to *cmt3 met1* mutants, which displayed a strong loss of H3 mK9 and a strong increase in H3 mK4. *PAI3* displayed a strong loss of H3 mK9 and a strong increase in H3 mK4 in *suvh4*, *cmt3*, and *cmt3 met1* mutants. The shifts from H3 mK9 to H3 mK4 at *PAI2* and *PAI3* in the DNA methylation-deficient strains mirror the degrees to which each gene is transcriptionally reactivated in each mutant background, as discussed above.

For controls for ChIP, we also monitored H3 mK9 and H3 mK4 at characterized loci representative of heterochromatin or euchromatin: the methylated and transcriptionally silent *Ta3* retrotransposon, the methylated and transcriptionally silent *AtMu1* DNA transposon, and the unmethylated and transcriptionally active *Actin* gene (14, 23). In agreement with a previous study (14), we found that *Ta3* had H3 mK9 in wild-type WS but was depleted for this modification in *suvh4*, *cmt3*, and *cmt3 met1* mutants (Fig. 2D). *Ta3* was enriched for H3 mK4 in *cmt3* and *cmt3 met1* mutants (Fig. 2D), the mutant backgrounds where the element is transcriptionally reactivated (14). Also in agreement with a previous study (23), we found that *AtMu1* had H3 mK9 and a low level of H3 mK4 in wild-type WS (Fig. 2D). *AtMu1* H3 mK9 was reduced in the *suvh4* mutant, but not in the *cmt3* mutant, without a change in H3 mK4 relative to the wild type. However, *AtMu1* lost H3 mK9 and acquired H3 mK4 in the *cmt3 met1* double mutant. The H3 mK4 methylation patterns are consistent with previously determined patterns of *AtMu1* transcriptional activity: the element is not activated in the *suvh4* and *cmt3* mutants but is

partially activated in the *met1* mutant (23). The *Actin* gene carried similar levels of H3 mK4 and no H3 mK9 in all four backgrounds assayed (Fig. 2E), demonstrating that the H3 mK4 pathway is not perturbed in DNA methylation-deficient mutants.

The *suvh4 suvh6* double mutant displays loss of H3 mK9 on the *PAI1-PAI4* transcribed inverted repeat. Because the H3 dimethyl K9 MTase activity of SUVH6 enzyme is similar to that of SUVH4 in vitro (10), we investigated whether SUVH6 acts at *PAI1-PAI4* in vivo by testing the effects of a *suvh6* mutation on WS *PAI* gene H3 methylation and DNA methylation. The *suvh6-1* mutation (hereafter referred to as *suvh6*) is a T-DNA insertion into the catalytic pre-SET-encoding domain of the gene isolated in the Col strain (Materials and Methods), likely creating a null allele. Col lacks a *PAI* inverted repeat and has unmethylated *PAI* genes (30). We therefore crossed the *suvh6* allele into a WS *pai1* reporter background, either as a single mutant or as a double mutant with an *suvh4* null allele. The WS *pai1* strain displays PAI-deficient phenotypes, including blue fluorescence under UV light, due to a missense mutation in the *PAI1* gene that impairs the major source of PAI enzyme from this constitutively transcribed locus without impairing the dsRNA signal for *PAI* DNA methylation (1). PAI-deficient phenotypes are suppressed when DNA methylation is reduced on the functional but silenced target gene *PAI2*, for example, in the *pai1 suvh4* and *pai1 cmt3* mutants (2, 25).

To determine the effects of the *suvh6* mutation on *PAI* H3 mK9, we performed ChIP for this modification, as well as for H3 mK4, in *suvh6* and *suvh4 suvh6* mutants with wild-type WS and the *suvh4* mutant for comparison. The *suvh6* mutant displayed a partial reduction, and the *suvh4 suvh6* double mutant displayed a stronger reduction in H3 mK9 at the *PAI1-PAI4* locus relative to the wild type and *suvh4* mutant (Fig. 3A). These data indicate that SUVH6 and SUVH4 both contribute to H3 mK9 at *PAI1-PAI4*, such that both enzymes must be inactivated before there is a substantial loss of the modification. There was only a low level of H3 mK4 at *PAI1-PAI4* in the *suvh6* and *suvh4 suvh6* mutant backgrounds, as observed for the wild type and *suvh4* and DNA MTase mutant backgrounds (Fig. 2A and 3A).

As discussed above, the singlet *PAI2* and *PAI3* genes are depleted for H3 mK9 in the *suvh4* mutant (Fig. 2C and 3B), suggesting that SUVH4 is the major contributor to H3 mK9 modification of these loci. Consistent with this view, *PAI2* and *PAI3* maintained H3 mK9 but not H3 mK4 in the *suvh6* mutant similar to the wild type (Fig. 3B). Furthermore, *PAI2* and *PAI3* H3 methylation patterns were similar in *suvh4 suvh6* and *suvh4* mutants (Fig. 3B).

The levels of H3 mK9 at the *Ta3* retrotransposon and the *AtMu1* DNA transposon in the wild type and *suvh4*, *suvh6*, and *suvh4 suvh6* mutants followed similar patterns to those seen at *PAI2* (Fig. 3B and C). H3 mK9 was maintained at both transposons in the wild type and *suvh6* mutant but was depleted in the *suvh4* mutant, indicating that SUVH4 is the major enzyme involved in modification of these loci. The *suvh4 suvh6* double mutant displayed H3 methylation patterns similar to those of the *suvh4* single mutant at both *Ta3* and *AtMu1*, suggesting that the role of SUVH6 at the transposons is minimal. *Actin* lacked H3 mK9 and carried similar high levels of H3 mK4 in

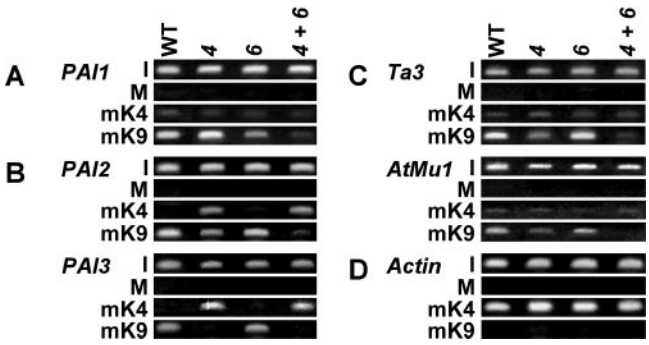

FIG. 3. *PAI* gene H3 mK4 and H3 mK9 patterning in *suvh6* and *suvh4 suvh6* mutants. Primer sets specific for (A) the *PAI-PAI4* transcribed inverted repeat, (B) the *PAI2* and *PAI3* targets for *PAI1-PAI4* RNA-directed DNA methylation, (C) the *Ta3* retrotransposon and *AtMu1* DNA transposon, and (D) the unmethylated transcribed *Actin* gene were used to amplify PCR products from total input chromatin (I), no-antibody mock precipitation control (M), chromatin immunoprecipitated with H3 anti-dimethyl K4 antibodies (mK4), or chromatin immunoprecipitated with H3 anti-dimethyl K9 antibodies (mK9) from the indicated strains. Four strains, wild-type WS (WT) and three mutants, were used. All mutations assayed were in the WS *pai1* background, with *4* indicating *suvh4*, *6* indicating *suvh6*, and *4 + 6* indicating *suvh4 suvh6*. GelStar-stained PCR products are shown. These results were reproduced in three independent experiments, with a representative data set shown.

suvh6 and *suvh4 suvh6* mutants, similar to all other mutants tested (Fig. 2D and 3D).

The *suvh4 suvh6* double mutant displays a loss of non-CG methylation on the *PAI1-PAI4* transcribed inverted repeat. The effect of the *suvh6* mutation on *PAI* DNA methylation was monitored by Southern blot analysis and by bisulfite genomic sequencing. For Southern blot analysis, genomic DNA was digested with HpaII, MspI, or HincII (Fig. 4A). The *suvh6* mutant displayed cleavage patterns at *PAI1-PAI4* similar to those of the *suvh4* mutant or wild-type WS. Thus, although H3 mK9 at *PAI1-PAI4* was partially reduced in the *suvh6* mutant compared to the levels in the mutant *suvh4* or wild-type WS (Fig. 3A), this intermediate level of modification is apparently sufficient to maintain high levels of non-CG methylation at the locus. The *suvh6* mutant also displayed cleavage patterns at *PAI2* and *PAI3* similar to those of wild-type WS (Fig. 4A). Correspondingly, the *suvh6* mutant maintained H3 mK9 at *PAI2* and *PAI3* at levels similar to those of wild-type WS (Fig. 3B). In addition, the *suvh6* mutant did not significantly alter the strong fluorescence phenotype diagnostic of *PAI2* silencing in the *pai1* reporter background (Fig. 5).

In contrast, the *suvh4 suvh6* double mutant displayed cleavage patterns diagnostic of reduced non-CG methylation on *PAI1-PAI4* compared to the WS, *suvh6*, or *suvh4* background (Fig. 4A). The reduced non-CG methylation corresponded to the strong loss of H3 mK9 observed at *PAI1-PAI4* in the *suvh4 suvh6* mutant (Fig. 3A). This result supports the view that SUVH4 and SUVH6 act in combination to maintain heterochromatin-associated epigenetic modifications at the *PAI1-PAI4* transcribed inverted repeat. However, the *suvh4 suvh6 PAI1-PAI4* demethylation patterns were slightly less complete than those observed in *cmt3* (Fig. 4A), suggesting that H3 K9

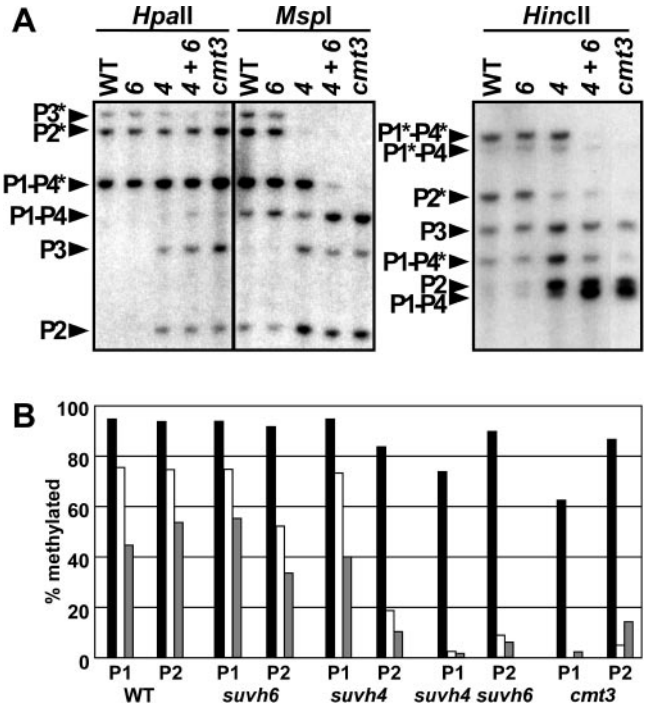

FIG. 4. The *suvh4 suvh6* double mutant displays loss of DNA methylation at the *PAI1-PAI4* inverted repeat. (A) Southern blot assays for *PAI* DNA methylation patterning in *suvh6* and *suvh4 suvh6* mutants. Genomic DNA from the indicated strains was cleaved with HpaII, MspI, or HincII and used in Southern blot analysis with a *PAI1* cDNA probe. P1-P4 indicates *PAI1-PAI4*, P2 indicates *PAI2*, and P3 indicates *PAI3*, with bands diagnostic of methylation on *PAI*-internal sites denoted with asterisks. All mutations assayed were in the WS *pai1* background, with WT indicating wild type for *SUVH4* and *SUVH6*, *4* indicating *suvh4*, *6* indicating *suvh6*, and *4 + 6* indicating *suvh4 suvh6*. (B) Bisulfite genomic sequencing of DNA methylation patterning on the *PAI1* and *PAI2* proximal promoters in *suvh6* and *suvh4 suvh6* mutants. Eight independent top-strand clones were sequenced for *PAI1* (P1) or *PAI2* (P2) from the same DNA samples used in panel A. The percentage of 5-methyl-cytosines out of total cytosines sequenced within the region of *PAI* sequence identity (344 bp for *PAI1* or 338 bp for *PAI2*) is shown, divided into the following contexts: CG (black), CNG (white), or other (gray). Data for wild-type WS (WT) and *cmt3* and *suvh4* mutants are from previous publications (2, 24, 25).

MTasesbesides SUVH4 and SUVH6 might contribute to modification of this locus.

The *suvh4 suvh6* double mutant displayed similar *PAI2* and *PAI3* cleavage patterns to those of the *suvh4* mutant, diagnostic of reduced non-CG methylation (Fig. 4A). In addition, *suvh6* did not significantly alter the intermediate fluorescence phenotype diagnostic of partial *PAI2* silencing in the *pai1 suvh4* background (Fig. 5).

To monitor *PAI* methylation patterning in detail, we performed bisulfite sequencing of the proximal promoter regions for *PAI1* and *PAI2* in the *suvh6* and *suvh4 suvh6* backgrounds (Fig. 4B). This analysis showed that the *suvh6* mutant carried substantial methylation in CG and non-CG sequence contexts for *PAI1*, similar to the wild-type WS or the *suvh4* mutant; the *suvh6* mutant carried substantial methylation in CG and non-CG sequence contexts for *PAI2*, similar to wild-type WS. The *suvh4 suvh6* double mutant retained substantial CG methylation but had a strong reduction in non-CG methylation on

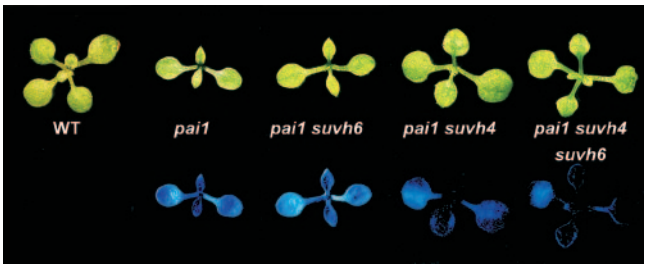

FIG. 5. The *suvh6* mutation does not suppress *PAI2* silencing. Representative 2-week-old seedlings of the indicated genotypes are shown photographed under visible light (top row) or short-wave UV light (bottom row). WT is wild-type WS.

PAI1 and *PAI2* relative to wild-type WS, similar to the *cmt3* mutant.

The *suvh6* mutation does not affect maintenance of non-CG methylation at centromere repeats and transposon sequences. Centromere repeats and transposons constitute major targets of non-CG methylation controlled by SUVH4 and CMT3, as indicated by increased MspI cleavage of these sequences in *suvh4* or *cmt3* backgrounds (11, 14, 23, 25). For example, in the wild type, MspI cleavage of the 180-bp centromere repeat sequence yields a ladder of bands that are shifted downwards in molecular weight partially in the *suvh4* mutant and more strongly in the *cmt3* mutant (11, 25). Similarly, the *Ta3* retrotransposon (11, 14) and the *AtMu1* DNA transposon (23) have partially increased MspI cleavage in the *suvh4* mutant and nearly complete MspI cleavage in the *cmt3* mutant. To assess the role of SUVH6 in maintenance of non-CG methylation on these sequences, we tested their MspI cleavage patterns in *suvh6* and *suvh4 suvh6* backgrounds. The *suvh6* single mutant displayed centromere repeat, *Ta3* (single copy), and *AtMu1* (three related methylated sequences detected in WS) digestion patterns similar to those of wild-type WS (Fig. 6). Correspondingly, the *suvh4 suvh6* double mutant displayed digestion patterns at these sequences similar to those of the *suvh4* single mutant, except that there was a slight enhancement of *AtMu1* cleavage in the double mutant. Thus, unlike SUVH4, the contribution of SUVH6 to the maintenance of centromere and transposon DNA methylation is minimal.

DISCUSSION

Previous studies including a genetic screen for maintenance of *PAI2* promoter methylation conducted in our laboratory identified the SUVH4 H3 K9 MTase as a factor in the maintenance of non-CG methylation patterning mediated by the *Arabidopsis* CMT3 DNA MTase (11, 25). SUVH4 also contributes to H3 dimethyl K9 genome-wide: the *suvh4* mutant displays a global loss of H3 mK9 as assessed by immunoblot analysis of total histones or by immunocytology (10, 12). Consistent with this global H3 mK9 depletion, ChIP analysis of specific heterochromatin targets, such as transposons, shows a loss of H3 mK9 in the *suvh4* mutant background relative to the wild-type background (14, 23) (Fig. 2D and 3C). However, transposons and centromere repeats retain residual non-CG methylation in a *suvh4* mutant background relative to a *cmt3* mutant background (11, 14, 23, 25) (Fig. 6), implying that

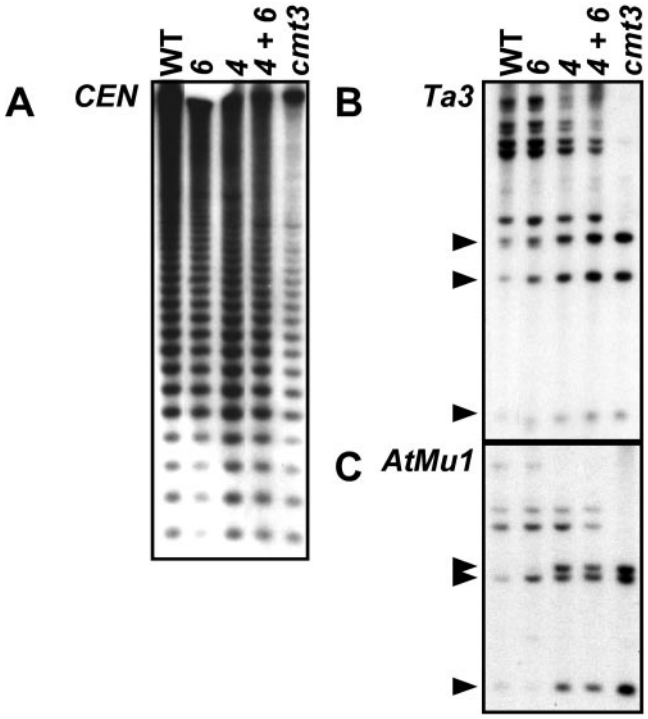

FIG. 6. Centromere and transposon non-CG methylation patterns in *suvh6* and *suvh4 suvh6* mutants. DNA from the indicated strains was cleaved with MspI (A and B) or HindIII plus MspI (C) and used in Southern blot analysis with a 180-bp centromere repeat sequence probe (*CEN*) (A), a *Ta3* probe (B), or an *AtMu1* probe (C). Arrowheads in the left margin indicate the positions of fully cleaved bands. All mutations assayed were in the WS *pai1* background, with WT indicating wild type for *SUVH4* and *SUVH6*, *4* indicating *suvh4*, *6* indicating *suvh6*, and *4 + 6* indicating *suvh4 suvh6*.

additional H3 K9 MTases might contribute to CMT3-mediated DNA methylation. Here we show the SUVH6 MTase is also active in maintaining H3 K9 and DNA methylation in vivo. Strikingly, the contribution of SUVH6 is locus dependent, with a major role in modification of the *PAI1-PAI4* transcribed inverted repeat, but not in modification of heterochromatin targets, including the *PAI2* duplication and transposon sequences (Fig. 2, 3, 4, and 6). Given the specificity of SUVH6 for H3 K9 in vitro (10), the simplest explanation of our results is that SUVH6 functions as an H3 K9 MTase in vivo. However, it is also possible that in vivo SUVH6 controls a different histone modification which has an indirect effect on H3 K9 and DNA methylation levels.

The *PAI1-PAI4* inverted repeat presents an unusual situation where the locus is both DNA methylated and transcriptionally active due to an upstream unmethylated promoter. Another unusual feature of the locus is that it produces a direct source of dsRNA that can potentially be processed in *cis* for very efficient recruitment of the RNA-directed heterochromatin machinery (29). Furthermore, unlike a highly transcribed inverted repeat transgene system for RNA-directed DNA methylation where non-CG methylation is maintained redundantly by CMT3 and DRM DNA MTases (5), CMT3 alone maintains the majority of non-CG methylation at *PAI1-PAI4* (2). The *PAI1-PAI4* inverted repeat thus provides a unique reporter locus to dissect the SUVH/CMT3 pathway uncomplicated by the DRM pathway. The basis for the difference between transgene inverted repeats and the endogenous *PAI1-PAI4* inverted repeat remains to be elucidated, but a possible explanation is that the much higher level of dsRNA produced in transgene systems more effectively recruits the DRM MTases. Alternatively, the lack of introns, polyadenylation sequences, or open reading frames in RNA produced from transgene constructs might feed the RNA into a different processing pathway than the *PAI1-PAI4* transcripts, leading to recruitment of different heterochromatin factors.

ChIP analysis of the *PAI1-PAI4* transcribed inverted repeat shows that it carries H3 methylation marks normally associated with transcriptionally silent heterochromatin: high levels of H3 mK9 and low levels of H3 mK4 (Fig. 2A). However, unmethylated *S15a*-derived sequences flanking *PAI1-PAI4*, including the *PAI1* transcription start site that lies approximately 500 bp upstream of the DNA methylated region, maintain H3 mK4 (Fig. 1A and 2B). These patterns suggest that heterochromatin formation signals localized to the palindromic *PAI-PAI4* sequences override the H3 mK4 mark of transcriptional activity. A similar heterochromatin override might occur at DNA methylated transposon and repeat sequences that are transcribed by read-through mechanisms.

The H3 mK9 modification is lost from *PAI1-PAI4* in the *cmt3 met1* double mutant strain but not in the *cmt3* single mutant strain (Fig. 2A). This loss is probably not due to transcriptional hyperactivation of the locus, since steady-state *PAI1* transcript levels are not significantly altered in the *cmt3 met1* mutant relative to the *cmt3* mutant (Fig. 1B). Analogously, plant transgenes with unmethylated promoters but methylated internal sequences do not display increased transcription initiation due to reductions in internal DNA methylation (8, 33). Instead, the loss of H3 mK9 in the *cmt3 met1* mutant suggests that dsRNA alone is not sufficient to maintain full H3 mK9 on the inverted repeat and that residual DNA methylation is also required. For example, DNA methylation could recruit RNA processing or binding factors that create a signal for H3 mK9 at the locus as a heterochromatin reinforcement mechanism. We do not currently have a means to test this possibility in the *PAI* system because *PAI* small RNAs are not detectable by conventional methods (29). However, other targets of RNA-directed DNA methylation, including transposons and 5S rRNA genes, display a reduction in small RNAs in a *met1* mutant background (23, 36), consistent with a reinforcing role of DNA methylation in maintenance of small RNAs for transcribed loci that are also heterochromatin targets. In a potentially related mechanism, methylation maintained by MET1 contributes to RNA interference triggered by a direct repeat transgene (32). Moreover, in fission yeast the initial RNA-induced H3 mK9 mark at heterochromatin targets subsequently serves to recruit the RNA effector complex that directs additional H3 mK9 for efficient maintenance of the modification (35).

In contrast to the transcribed *PAI1-PAI4* inverted repeat, the silenced *PAI2* and *PAI3* target loci display loss of H3 mK9 and gain of H3 mK4 in parallel to their transcriptional reactivation patterns induced by DNA demethylation. For example, *PAI2* is partially reactivated in the *cmt3* mutant background and fully reactivated in the *cmt3 met1* mutant background on

the basis of the phenotypes observed in the *pai1* reporter strain for *PAI2* silencing (2) (Materials and Methods); correspondingly, *PAI2* displays a partial loss of H3 mK9 and partial gain of H3 mK4 in the *cmt3* mutant and a complete loss of H3 mK9 and strong gain of H3 mK4 in the *cmt3 met1* mutant (Fig. 2C). *PAI3* has minimal promoter methylation compared to *PAI2* (24); correspondingly, *PAI3* displays complete loss of H3 mK9 and strong gain of H3 mK4 in both the *cmt3* mutant and *cmt3 met1* mutant (Fig. 2C). These patterns thus support the view that the RNA signal for heterochromatin produced from the *PAI1-PAI4* locus is not efficient enough acting in *trans* on *PAI2* and *PAI3* to affect H3 mK4 directed by transcriptional activation.

Our analysis of *PAI* H3 mK9 patterning in *suvh4*, *suvh6*, and *suvh4 suvh6* mutant backgrounds indicates that SUVH4 and SUVH6 together control modification of *PAI1-PAI4*: both enzymes must be inactivated before there is a loss of H3 mK9 sufficient for loss of non-CG methylation from the locus (Fig. 3A and 4). In contrast, SUVH6 does not significantly contribute to H3 mK9 (Fig. 3), DNA methylation patterning (Fig. 4), or transcriptional silencing (Fig. 5) at *PAI2*. Because DNA sequences and DNA methylation patterns are nearly identical between *PAI1-PAI4* and *PAI2* (24), these features are unlikely to mediate the preferential activity of SUVH6 at *PAI1-PAI4*. Instead, an obvious distinction is that *PAI1-PAI4* is transcribed to produce dsRNA, whereas *PAI2* is a transcriptionally silent target of the dsRNA (29). Thus, SUVH6 and SUVH4 could both be efficiently recruited to *PAI1-PAI4* by a unique species of RNA processing or effector complex that assembles in *cis* at this transcribed inverted repeat. In this view, *PAI2* and *PAI3* would be associated with a different *trans*-acting RNA effector complex that preferentially recruits SUVH4. Similarly, transposon targets for DNA methylation do not produce transcripts that directly form dsRNA, and instead probably generate dsRNA indirectly through RNA-dependent RNA polymerase-mediated mechanisms (8, 33, 43). Therefore, transposons might also be associated with RNA effector complexes that preferentially recruit SUVH4. An alternative view is that SUVH6 is preferentially recruited to *PAI1-PAI4* through DNA features unique to this locus, such as a higher-order assembly formed by the inverted repeat. Future experiments that dissect the expression and structural and functional differences between SUVH4 and SUVH6 will clarify the mechanisms underlying histone MTase targeting in RNA-directed heterochromatin formation.

In fission yeast the RITS effector complex, which includes an argonaute small RNA binding protein, mediates the recruitment of H3 mK9 to heterochromatin target regions (42). Functionally analogous effector complexes are also presumed to exist in plants, but their components have so far eluded detection in genetic screens, perhaps because of genetic redundancy. For example, *Arabidopsis* encodes 10 argonaute proteins (31). However, if SUVH6 is preferentially recruited to *PAI1-PAI4* through affinity for a unique RNA effector complex that assembles at the locus, the SUVH6/*PAI1-PAI4* system could allow genetic and molecular identification of new factors in the RNA-directed heterochromatin system despite redundancy at other heterochromatic loci.

Our finding that the *suvh4 suvh6* double mutant displays enhanced non-CG demethylation at *PAI1-PAI4* relative to the *suvh4* mutant shows that CMT3-mediated DNA methylation depends on H3 mK9 controlled by partially redundant histone MTase activities. The residual non-CG methylation at *PAI*, transposon, and centromere repeat sequences in the *suvh4 suvh6* mutant versus the *cmt3* mutant (Fig. 4A and 6) suggests that H3 K9 MTases in addition to SUVH4 and SUVH6, such as the other seven SUVH proteins encoded in *Arabidopsis* (3), also contribute to maintenance of DNA methylation at these regions. For example, SUVH2 was recently characterized in vitro and in vivo as having H3 K9 MTase activity (34). An alternative view to account for the residual non-CG methylation in the *suvh4* mutant versus the *cmt3* mutant is that CMT3 might be recruited with reduced efficiency to target sequences by an H3 mK9-independent mechanism. For example, in vitro evidence suggests that CMT3 acts by combined recognition of H3 mK9 and H3 m27 marks (21). It is also possible that the *suvh6-1* allele used in this analysis retains partial activity. However, given that the insertional disruption in this allele splits the essential catalytic pre-SET domain sequences away from the SET and post-SET domain sequences, this possibility is unlikely. Analysis of additional *suvh* mutations in combination with *suvh4* and *suvh6* will indicate whether residual non-CG methylation is controlled by other SUVH histone MTases.

ACKNOWLEDGMENTS

We thank Thomas Jenuwein (Vienna Biocenter) for H3 antidimethyl K9 antibodies, Syngenta (Research Triangle Park, North Carolina) for the *suvh6-1* T-DNA insertion mutant, and Eric Richards (Washington University, St. Louis, Mo.) for the *met1-1* mutant.

This work was supported by National Institutes of Health grant GM61148 to J.B. and by training grants NIEHS T32 ES007141 and NCI T32 CA09110 to M.L.E.

REFERENCES

1. **Bartee, L., and J. Bender.** 2001. Two *Arabidopsis* methylation-deficiency mutations confer only partial effects on a methylated endogenous gene family. Nucleic Acids Res. **29:**2127–2134.
2. **Bartee, L., F. Malagnac, and J. Bender.** 2001. *Arabidopsis cmt3* chromomethylase mutations block non-CG methylation and silencing of an endogenous gene. Genes Dev. **15:**1753–1758.
3. **Baumbusch, L. O., T. Thorstensen, V. Krauss, A. Fischer, K. Naumann, R. Assalkhou, I. Schulz, G. Reuter, and R. B. Aalen.** 2001. The *Arabidopsis thaliana* genome contains at least 29 active genes encoding SET domain proteins that can be assigned to four evolutionarily conserved classes. Nucleic Acids Res. **29:**4319–4333.
4. **Bender, J., and G. R. Fink.** 1995. Epigenetic control of an endogenous gene family is revealed by a novel blue fluorescent mutant of *Arabidopsis*. Cell **83:**725–734.
5. **Cao, X., W. Aufsatz, D. Zilberman, M. F. Mette, M. S. Huang, M. Matzke, and S. E. Jacobsen.** 2003. Role of the DRM and CMT3 methyltransferases in RNA-directed DNA methylation. Curr. Biol. **13:**2212–2217.
6. **Cao, X., and S. E. Jacobsen.** 2002. Locus-specific control of asymmetric and CpNpG methylation by the *DRM* and *CMT3* methyltransferase genes. Proc. Natl. Acad. Sci. USA **99**(Suppl. 4)**:**16491–16498.
7. **Cao, X., and S. E. Jacobsen.** 2002. Role of the *Arabidopsis DRM* methyltransferases in de novo DNA methylation and gene silencing. Curr. Biol. **12:**1138–1144.
8. **Dalmay, T., A. Hamilton, S. Rudd, S. Angell, and D. C. Baulcombe.** 2000. An RNA-dependent RNA polymerase gene in *Arabidopsis* is required for posttranscriptional gene silencing mediated by a transgene but not by a virus. Cell **101:**543–553.
9. **Gendrel, A. V., Z. Lippman, C. Yordan, V. Colot, and R. A. Martienssen.** 2002. Dependence of heterochromatic histone H3 methylation patterns on the *Arabidopsis* gene *DDM1*. Science **297:**1871–1873.
10. **Jackson, J. P., L. Johnson, Z. Jasencakova, X. Zhang, L. PerezBurgos, P. B. Singh, X. Cheng, I. Schubert, T. Jenuwein, and S. E. Jacobsen.** 2004. Dimethylation of histone H3 lysine 9 is a critical mark for DNA methylation and gene silencing in *Arabidopsis thaliana*. Chromosoma **112:**308–315.
11. **Jackson, J. P., A. M. Lindroth, X. Cao, and S. E. Jacobsen.** 2002. Control of CpNpG DNA methylation by the KRYPTONITE histone H3 methyltransferase. Nature **416:**556–560.

12. **Jasencakova, Z., W. J. Soppe, A. Meister, D. Gernand, B. M. Turner, and I. Schubert.** 2003. Histone modifications in *Arabidopsis*—high methylation of H3 lysine 9 is dispensable for constitutive heterochromatin. Plant J. **33:**471–480.
13. **Jeddeloh, J. A., J. Bender, and E. J. Richards.** 1998. The DNA methylation locus *DDM1* is required for maintenance of gene silencing in *Arabidopsis*. Genes Dev. **12:**1714–1725.
14. **Johnson, L., X. Cao, and S. Jacobsen.** 2002. Interplay between two epigenetic marks. DNA methylation and histone H3 lysine 9 methylation. Curr. Biol. **12:**1360–1367.
15. **Johnson, L., S. Mollah, B. A. Garcia, T. L. Muratore, J. Shabanowitz, D. F. Hunt, and S. E. Jacobsen.** 2004. Mass spectrometry analysis of *Arabidopsis* histone H3 reveals distinct combinations of post-translational modifications. Nucleic Acids Res. **32:**6511–6518.
16. **Kankel, M. W., D. E. Ramsey, T. L. Stokes, S. K. Flowers, J. R. Haag, J. A. Jeddeloh, N. C. Riddle, M. L. Verbsky, and E. J. Richards.** 2003. *Arabidopsis MET1* cytosine methyltransferase mutants. Genetics **163:**1109–1122.
17. **Kato, M., A. Miura, J. Bender, S. E. Jacobsen, and T. Kakutani.** 2003. Role of CG and non-CG methylation in immobilization of transposons in *Arabidopsis*. Curr. Biol. **13:**421–426.
18. **Kouzminova, E., and E. U. Selker.** 2001. *dim-2* encodes a DNA methyltransferase responsible for all known cytosine methylation in *Neurospora*. EMBO J. **20:**4309–4323.
19. **Lehnertz, B., Y. Ueda, A. A. Derijck, U. Braunschweig, L. Perez-Burgos, S. Kubicek, T. Chen, E. Li, T. Jenuwein, and A. H. Peters.** 2003. *Suv39h*-mediated histone H3 lysine 9 methylation directs DNA methylation to major satellite repeats at pericentric heterochromatin. Curr. Biol. **13:**1192–1200.
20. **Lindroth, A. M., X. Cao, J. P. Jackson, D. Zilberman, C. M. McCallum, S. Henikoff, and S. E. Jacobsen.** 2001. Requirement of CHROMOMETHYLASE3 for maintenance of CpXpG methylation. Science **292:**2077–2080.
21. **Lindroth, A. M., D. Shultis, Z. Jasencakova, J. Fuchs, L. Johnson, D. Schubert, D. Patnaik, S. Pradhan, J. Goodrich, I. Schubert, T. Jenuwein, S. Khorasanizadeh, and S. E. Jacobsen.** 2004. Dual histone H3 methylation marks at lysines 9 and 27 required for interaction with CHROMOMETHYLASE3. EMBO J. **23:**4286–4296.
22. **Lippman, Z., A. V. Gendrel, M. Black, M. W. Vaughn, N. Dedhia, W. R. McCombie, K. Lavine, V. Mittal, B. May, K. D. Kasschau, J. C. Carrington, R. W. Doerge, V. Colot, and R. Martienssen.** 2004. Role of transposable elements in heterochromatin and epigenetic control. Nature **430:**471–476.
23. **Lippman, Z., B. May, C. Yordan, T. Singer, and R. Martienssen.** 2003. Distinct mechanisms determine transposon inheritance and methylation via small interfering RNA and histone modification. PLoS Biol. **1:**E67.
24. **Luff, B., L. Pawlowski, and J. Bender.** 1999. An inverted repeat triggers cytosine methylation of identical sequences in *Arabidopsis*. Mol. Cell **3:**505–511.
25. **Malagnac, F., L. Bartee, and J. Bender.** 2002. An *Arabidopsis* SET domain protein required for maintenance but not establishment of DNA methylation. EMBO J. **21:**6842–6852.
26. **Mathieu, O., and J. Bender.** 2004. RNA-directed DNA methylation. J. Cell Sci. **117:**4881–4888.
27. **McElver, J., I. Tzafrir, G. Aux, R. Rogers, C. Ashby, K. Smith, C. Thomas, A. Schetter, Q. Zhou, M. A. Cushman, J. Tossberg, T. Nickle, J. Z. Levin, M. Law, D. Meinke, and D. Patton.** 2001. Insertional mutagenesis of genes required for seed development in *Arabidopsis thaliana*. Genetics **159:**1751–1763.
28. **Melquist, S., and J. Bender.** 2004. An internal rearrangement in an *Arabidopsis* inverted repeat locus impairs DNA methylation triggered by the locus. Genetics **166:**437–448.
29. **Melquist, S., and J. Bender.** 2003. Transcription from an upstream promoter controls methylation signaling from an inverted repeat of endogenous genes in *Arabidopsis*. Genes Dev. **17:**2036–2047.
30. **Melquist, S., B. Luff, and J. Bender.** 1999. *Arabidopsis PAI* gene arrangements, cytosine methylation and expression. Genetics **153:**401–413.
31. **Morel, J. B., C. Godon, P. Mourrain, C. Béclin, S. Boutet, F. Feuerbach, F. Proux, and H. Vaucheret.** 2002. Fertile hypomorphic *ARGONAUTE* (*ago1*) mutants impaired in post-transcriptional gene silencing and virus resistance. Plant Cell **14:**629–639.
32. **Morel, J. B., P. Mourrain, C. Béclin, and H. Vaucheret.** 2000. DNA methylation and chromatin structure affect transcriptional and post-transcriptional transgene silencing in *Arabidopsis*. Curr. Biol. **10:**1591–1594.
33. **Mourrain, P., C. Béclin, T. Elmayan, F. Feuerbach, C. Godon, J. B. Morel, D. Jouette, A. M. Lacombe, S. Nikic, N. Picault, K. Remoue, M. Sanial, T. A. Vo, and H. Vaucheret.** 2000. *Arabidopsis* SGS2 and SGS3 genes are required for posttranscriptional gene silencing and natural virus resistance. Cell **101:**533–542.
34. **Naumann, K., A. Fischer, I. Hofmann, V. Krauss, S. Phalke, K. Irmler, G. Hause, A. C. Aurich, R. Dorn, T. Jenuwein, and G. Reuter.** 2005. Pivotal role of AtSUVH2 in heterochromatic histone methylation and gene silencing in *Arabidopsis*. EMBO J. **24:**1418–1429.
35. **Noma, K., T. Sugiyama, H. Cam, A. Verdel, M. Zofall, S. Jia, D. Moazed, and S. I. Grewal.** 2004. RITS acts in *cis* to promote RNA interference-mediated transcriptional and post-transcriptional silencing. Nat. Genet. **36:**1174–1180.
36. **Onodera, Y., J. R. Haag, T. Ream, P. C. Nunes, O. Pontes, and C. S. Pikaard.** 2005. Plant nuclear RNA polymerase IV mediates siRNA and DNA methylation-dependent heterochromatin formation. Cell **120:**613–622.
37. **Saze, H., O. M. Scheid, and J. Paszkowski.** 2003. Maintenance of CpG methylation is essential for epigenetic inheritance during plant gametogenesis. Nat. Genet. **34:**65–69.
38. **Soppe, W. J., Z. Jasencakova, A. Houben, T. Kakutani, A. Meister, M. S. Huang, S. E. Jacobsen, I. Schubert, and P. F. Fransz.** 2002. DNA methylation controls histone H3 lysine 9 methylation and heterochromatin assembly in *Arabidopsis*. EMBO J. **21:**6549–6559.
39. **Tamaru, H., and E. U. Selker.** 2001. A histone H3 methyltransferase controls DNA methylation in *Neurospora crassa*. Nature **414:**277–283.
40. **Tariq, M., H. Saze, A. V. Probst, J. Lichota, Y. Habu, and J. Paszkowski.** 2003. Erasure of CpG methylation in *Arabidopsis* alters patterns of histone H3 methylation in heterochromatin. Proc. Natl. Acad. Sci. USA **100:**8823–8827.
41. **Tompa, R., C. M. McCallum, J. Delrow, J. G. Henikoff, B. van Steensel, and S. Henikoff.** 2002. Genome-wide profiling of DNA methylation reveals transposon targets of CHROMOMETHYLASE3. Curr. Biol. **12:**65–68.
42. **Verdel, A., S. Jia, S. Gerber, T. Sugiyama, S. Gygi, S. I. Grewal, and D. Moazed.** 2004. RNAi-mediated targeting of heterochromatin by the RITS complex. Science **303:**672–676.
43. **Xie, Z., L. K. Johansen, A. M. Gustafson, K. D. Kasschau, A. D. Lellis, D. Zilberman, S. E. Jacobsen, and J. C. Carrington.** 2004. Genetic and functional diversification of small RNA pathways in plants. PLoS Biol. **2:**E104.
44. **Xin, Z., M. Tachibana, M. Guggiari, E. Heard, Y. Shinkai, and J. Wagstaff.** 2003. Role of histone methyltransferase G9a in CpG methylation of the Prader-Willi syndrome imprinting center. J. Biol. Chem. **278:**14996–15000.